Coherent Picture on the Pure Spin Transport between Ag/Bi and Ferromagnets

J. Cheng,[1,*] B. F. Miao,[1,2,*,†] Z. Liu,[3,*] M. Yang,[1] K. He,[1] Y. L. Zeng,[1] H. Niu,[1] X. Yang,[1] Z. Q. Wang,[1] X. H. Hong,[1] S. J. Fu,[1] L. Sun,[1,2] Y. Liu,[3] Y. Z. Wu,[2,4] Z. Yuan,[3,‡] and H. F. Ding[1,2,§]

[1]*National Laboratory of Solid State Microstructures and Department of Physics, Nanjing University, Nanjing 210093, People's Republic of China*

[2]*Collaborative Innovation Center of Advanced Microstructures, Nanjing University, Nanjing 210093, People's Republic of China*

[3]*Center for Advanced Quantum Studies and Department of Physics, Beijing Normal University, Beijing 100875, People's Republic of China*

[4]*Department of Physics, Fudan University, 220 Handan Road, Shanghai 200433, People's Republic of China*

(Received 25 January 2022; accepted 26 July 2022; published 24 August 2022)

In a joint effort of both experiments and first-principles calculations, we resolve a hotly debated controversy and provide a coherent picture on the pure spin transport between Ag/Bi and ferromagnets. We demonstrate a strong inverse Rashba-Edelstein effect (IREE) at the interface in between Ag/Bi with a ferromagnetic metal (FM) but not with a ferromagnetic insulator. This is in sharp contrast to the previously claimed IREE at Ag/Bi interface or inverse spin Hall effect dominated spin transport. A more than one order of magnitude modulation of IREE signal is realized for different Ag/Bi-FM interfaces, casting strong tunability and a new direction for searching efficient spintronics materials.

DOI: 10.1103/PhysRevLett.129.097203

Spin-orbit coupling (SOC), which describes the entanglement of electrons' spin and orbital degrees of freedom, is the central ingredient of modern condensed matter physics [1,2]. It plays pivotal roles in the formation of topological band structures [3,4] and topological spin textures [5], as well as in spin-charge interconversions [2,6,7]. In bulk materials, SOC enables the generation and detection of pure spin current through the spin Hall effect (SHE) [8,9] and inverse spin Hall effect (ISHE) [10,11], respectively. These reciprocal effects have been widely used in the spin Hall nano-oscillators [12,13], spin-orbit torque-induced magnetization switching [14–16], spin pumping measurements [10,17–21], etc. At the surface or interface with broken inversion symmetry, Rashba SOC emerges with a spin-dependent band splitting featured with spin-momentum locking [1,6]. Consequently, the flow of an in-plane charge current in the Rashba system also generates a pure spin current in its transverse direction and vice versa. These are the Rashba-Edelstein effect (REE) [22] and the inverse Rashba-Edelstein effect (IREE) [23], respectively.

Recently, there has been a hot debate on the mechanism of the pure spin transport in Ag/Bi related systems [24–35]. Utilizing a ferromagnetic metal (FM) permalloy (Py) as the spin injector, Sánchez *et al.* first reported the observation of the IREE at Ag/Bi interface using spin pumping measurements [24]. They observed a large enhancement of the converted charge current in Ag/Bi bilayer as compared to a Bi or Ag single layer and attributed it to the IREE at the Ag/Bi interface. This seminal work stimulated hot discussions about pure spin transport in Ag/Bi bilayers [25–34]. However, a relatively weaker signal was found when a ferromagnetic insulator (FI) $Y_3Fe_5O_{12}$ (YIG) was selected as the spin current source [30], whereas no sign change was observed with reversing stacking order of Ag and Bi, inconsistent with the IREE scenario [30]. In addition, thermal injection of spin current from YIG into both Bi and Ag/Bi bilayer results in only negligibly small spin-charge conversion [33,35]. Very recently, Shen *et al.* performed a spin-charge conversion study in the Ag/Bi bilayer by spin pumping with two spin current sources, namely, Fe/Ag/Bi/Py multilayer, and attributed it to the ISHE rather than the IREE [34]. The considerable controversy calls for a comprehensive study of the Ag/Bi related spin-charge conversion.

In this Letter, utilizing spin pumping, we report a systematic study of the spin-charge conversion in systems of Ag/Bi in contact with various FMs (Fe, Ni, and FeNi alloy) and a FI (YIG) and sandwiched between them. We unambiguously identified the IREE at the interface between Ag/Bi and FMs, rather than the previously claimed IREE at Ag/Bi interface or ISHE-dominated pure spin transport. Our findings not only are supported by both our experiments and first-principles calculations, but also reconcile almost all the published experimental data in the literature with controversial conclusions. Thus, it provides a coherent picture on the pure spin transport between Ag/Bi and ferromagnets. In addition, we find that the amplitude of the IREE can be tuned with more than one order of magnitude for Ag/Bi in contact with different FMs. The strong

tunability points a new direction for searching spintronics materials with high efficiency.

For the ISHE, the converted charge current density $\vec{j}_C$ can be described by

$$\vec{j}_C = \theta_{\mathrm{SH}}(2e/\hbar)\vec{j}_S \times \vec{\sigma},$$

where θ_{SH} is the spin Hall angle of the materials and $\vec{j}_S$ is the spin current density with its spin polarization $\vec{\sigma}$. Thus, reversing the flow direction of $\vec{j}_S$ while maintaining its polarization results in a sign change of $\vec{j}_C$. On the other hand, the charge current associated with the IREE is

$$\vec{j}_C = \alpha_R(2e/\hbar)\vec{z} \times \vec{S}.$$

Here, α_R is the Rashba coefficient, $\vec{S}$ is the nonequilibrium spin density due to the spin injection, and $\vec{z}$ is the direction vector along the Rashba electric field (typically normal to the interface) [24,34]. As the sign of the Rashba electric field depends on the stacking order of the two layers adjacent to the interface, $\vec{j}_C$ reverses its sign when the stacking order is flipped. This is generally considered as the fingerprint of the IREE and has been used to distinguish it from ISHE [36]. In addition, due to the spin-momentum locking, $\vec{j}_C$ depends on only the spin polarization of the pure spin current but is irrelevant with its flow direction. Considering the Ag/Bi bilayer sandwiched by two ferromagnets, i.e., F1/Ag/Bi/F2, spin current can be injected from either side to Ag/Bi interface under their different resonance conditions [Fig. 1(a)]. The spin pumping curve is expected to exhibit a "double-peak" ("peak-and-dip") feature if IREE at Ag/Bi interface (ISHE) is the dominant mechanism for the spin-charge conversion [Fig. 1(b)]. This approach was first proposed by Shen *et al.* and used as the criterion to distinguish IREE and ISHE recently [34].

Figure 1(c) presents the measured spin pumping signal for Fe(10)/Ag(5)/Bi(6)/Py(10) (the numbers in parentheses represent their thicknesses in units of nanometers). For the details of the sample preparation, measurements, and x-ray diffraction, see Supplemental Material [37], Note 1. Consistent with Ref. [34], we also observed a peak-and-dip feature. The current changes sign with reversing the magnetic field, reflecting its pure spin current origin. Based on the aforementioned criterion, one may draw the conclusion that the spin-charge conversion herein is conducted mainly through the ISHE of Ag/Bi bilayer. However, we observed a completely different behavior when the metallic Fe is replaced with YIG, a FI. A double peak appears in YIG/Ag/Bi/Py multilayers [Fig. 1(d)]. The opposite conclusion may be drawn based on the above-mentioned criterion.

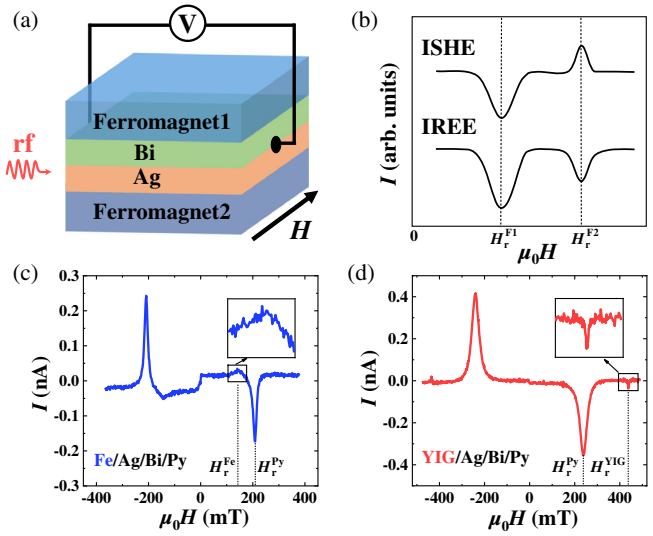

FIG. 1. (a) Schematic illustration of spin pumping measurement for Ag/Bi bilayer sandwiched by two different ferromagnets. Under their different resonance conditions, the spin current can be injected into Ag/Bi from either side. (b) Spin currents injected from opposite directions result in the same (opposite) sign of charge currents in the IREE (ISHE) mechanism, with a double-peak (peak-and-dip) feature. Spin pumping signals at the frequency of 14 GHz for (c) Fe(10)/Ag(5)/Bi(6)/Py(10) and (d) YIG/Ag(5)/Bi(6)/Py(10), respectively.

The opposite feature of spin pumping signals in Fe/Ag/Bi/Py and YIG/Ag/Bi/Py multilayers indicates that the ferromagnetic layer itself or the interface between Ag/Bi and ferromagnet may also have a strong impact on the results. In the following, we will discuss these two influences one by one. It has been recognized that FM not only can act as a spin current source, but also can serve as a spin detector to probe spin current via ISHE [45,46]. Thus, the spin-charge conversion in FMs may complicate the analysis. To minimize this influence, one need to find a FM with $\theta_{\mathrm{SH}} \approx 0$. Fortunately, Fe and Ni have negative and positive θ_{SH} [46], respectively. FeNi alloy, thus, provides a platform to tailor the effective θ_{SH} by controlling the relative concentration. Figure 2(a) presents the spin pumping curves for YIG/$Fe_{1-x}Ni_x$(10) bilayers with different concentrations. The negligibly small signal in YIG/$Fe_{0.65}Ni_{0.35}$ bilayer indicates $\theta_{\mathrm{SH}} \approx 0$ at $x = 0.35$. We, thus, further fabricate the YIG/Ag(5)/Bi(6)/$Fe_{0.65}Ni_{0.35}$(10) multilayers where the spin-charge conversion in the ferromagnetic layer itself is minimized. Interestingly, YIG/Ag/Bi/$Fe_{0.65}Ni_{0.35}$ still exhibits a double-peak feature [Fig. 2(b), top panel], evidencing that the ISHE in ferromagnetic metal plays a minor role in the samples studied here.

In the following, we continue our discussion on the interface effect. In the past, tremendous attention has been focused on the Ag/Bi interface, while the interface between ferromagnet and Ag/Bi bilayer was basically

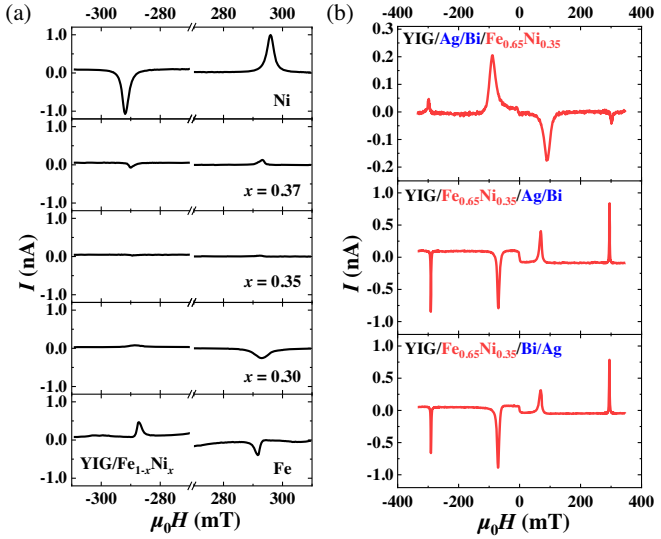

FIG. 2. (a) Spin pumping signals for YIG/$Fe_{1-x}Ni_x$(10) bilayers, with x varying from 0 to 1. The resonance signal vanishes at $x = 0.35$, evidencing $\theta_{SH} \approx 0$ for $Fe_{0.65}Ni_{0.35}$. (b) Spin pumping signals for YIG/Ag(5)/Bi(6)/$Fe_{0.65}Ni_{0.35}$(10) (top), YIG/$Fe_{0.65}Ni_{0.35}$(7)/Ag(5)/Bi(6) (middle), and YIG/$Fe_{0.65}Ni_{0.35}$(7)/Bi(6)/Ag(5) (bottom).

overlooked. In order to unveil the intriguing spin-charge conversion in an Ag/Bi related system, it is imperative to carefully investigate each interface in the YIG/Ag/Bi/FM multilayers. Figure 3(a) presents the spin pumping signals for Py(10)/Bi(11) and YIG/Bi(11) bilayers under a positive magnetic field [11-nm thickness Bi is chosen to maintain the same total thickness with Ag(5)/Bi(6)]. Similar to the observations in the literature [47,48], the charge current in Py/Bi is almost one order of magnitude larger than that in YIG/Bi. This, however, is counterintuitive, as typically YIG possesses much higher spin pumping efficiency. We also observed negligibly small signals in both YIG/Ag(5)/Bi(6) and YIG/Bi(6)/Ag(5),

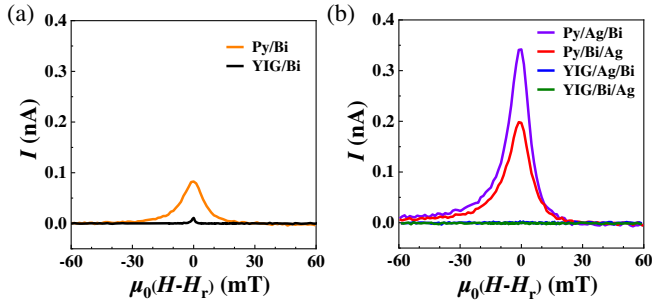

FIG. 3. (a) Spin pumping curves for Py(10)/Bi(11) (orange) and YIG/Bi(11) (black). (b) Spin pumping curves for Py(10)/Ag(5)/Bi(6) (purple), Py(10)/Bi(6)/Ag(5) (red), YIG/Ag(5)/Bi(6) (blue), and YIG/Bi(6)/Ag(5) (green). An almost vanishing signal is obtained with insulating YIG as the spin source, while an enhanced signal can be found by using metallic Py as the spin source.

in line with the results obtained with thermal injection [33]. This indicates negligibly small IREE and ISHE in both Ag/Bi and Bi/Ag bilayers [Fig. 3(b)]. On the other hand, strongly enhanced signals were obtained in Py(10)/Ag(5)/Bi(6) and Py(10)/Bi(6)/Ag(5) [Fig. 3(b)]. The contradictory behavior in the spin pumping measurements of Bi and Ag/Bi systems in contact with YIG and Py has been a long-lasting puzzle and remains unsolved. In addition, it is worth noting that the polarity of the spin pumping signals of Py/Bi, Py/Ag/Bi, and Py/Bi/Ag are opposite to that of YIG/Ag/Bi/Py at the resonance condition of YIG. Opposite signs of the obtained charge current with an identical spin current direction indicates that the spin-charge conversion in these systems unlikely relates to the ISHE in possible alloy of Ag/Bi or Ag/Bi with Py. Instead, it can be well explained by the IREE at the interface between Bi or Ag/Bi and Py. And the sign change between Py/Bi/Ag and YIG/Ag/Bi/Py is due to the reversed stacking order of Ag/Bi with Py. To further confirm this, we also reverse the stacking order of Ag/Bi and $Fe_{0.65}Ni_{0.35}$ and perform the control measurement with YIG/$Fe_{0.65}Ni_{0.35}$/Ag/Bi and YIG/$Fe_{0.65}Ni_{0.35}$/Bi/Ag as compared to YIG/Bi/Ag/$Fe_{0.65}Ni_{0.35}$. As shown in the middle and bottom panels in Fig. 2(b), the spin-charge conversions at both YIG and $Fe_{0.65}Ni_{0.35}$ resonance conditions reverse their sign as compared to YIG/Ag/Bi/$Fe_{0.65}Ni_{0.35}$, which again evidences the IREE at the interface between Ag/Bi and $Fe_{0.65}Ni_{0.35}$. We note that the slight difference between the signals at positive and negative fields at $Fe_{0.65}Ni_{0.35}$ resonance conditions is due to the planar Hall-effect-induced spin rectification [49], while the potential artifact from thermal signals is negligible in the spin pumping measurements [50]. Based on the above observations, we unambiguously identify the IREE at the interface between Ag/Bi and $Fe_{0.65}Ni_{0.35}$. To verify the generality of the observed IREE between Ag/Bi and FM and to demonstrate its tunability, we further performed the spin pumping measurements with a series of YIG/Ag/Bi/FMs, where FMs refer to the metallic Fe, $Fe_{0.65}Ni_{0.35}$, Py, and Ni, and found they varied with different FMs (Supplemental Material [37], Note 3). Especially, the spin pumping signal at the resonance condition of YIG is almost one order of magnitude larger in YIG/Bi/Ag/Ni than those in the other systems. And we also discussed the spin diffusion lengths in Bi and $Fe_{0.65}Ni_{0.35}$ layers (Supplemental Material [37], Note 4).

With the understanding of the IREE at Ag/Bi-FM interfaces, we now provide a possible explanation for the peak-and-dip feature observed in the Fe/Ag/Bi/Py as presented in Fig. 1(c). In this multilayer with double FMs as the spin sources, due to the spin diffusion, it can be anticipated that Fe/Bi(Ag) and Bi(Ag)/Py interface plays a major role in the spin-charge conversion when spin current is injected from the Fe and Py side, respectively. It is important to note that the Rashba coefficient of Fe/Bi(Ag) interface is opposite to that of Bi(Ag)/Py interface with comparable amplitude (Fig. S3 [37]), as

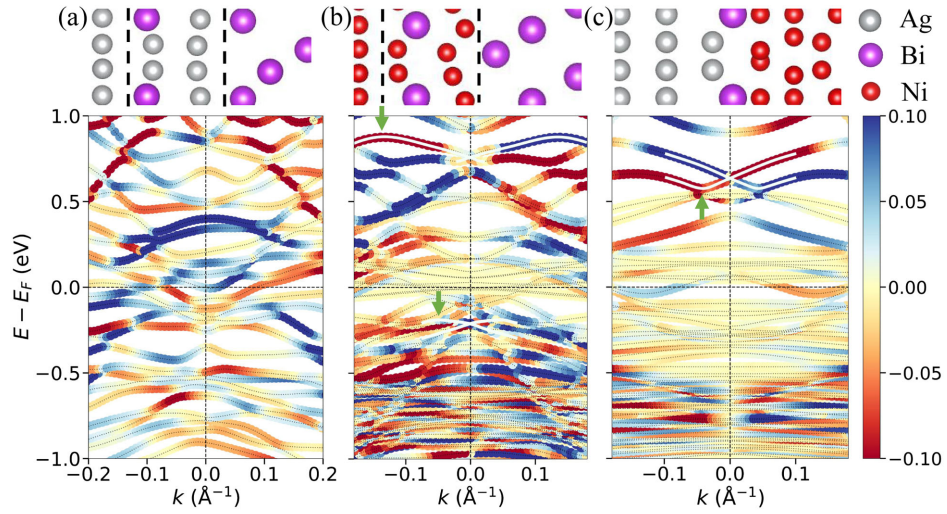

FIG. 4. Spin-projected band structures along $K - \Gamma - K$ ($k_y \equiv 0$) in the two-dimensional Brillouin zone for three different interfaces: (a) disordered Ag/Bi interface, (b) disordered Ni/Bi interface, and (c) Bi-doped Ag/Ni interface. The top panels illustrate the corresponding atomic structure at the interfaces. To model the interfacial disorder, a $\sqrt{3} \times \sqrt{3}$ supercell of the (111) Ag (Ni) surface is used, and the atoms in the interfacial layers (between the two black dashed lines) are allowed to be randomly occupied by Ag (Ni) and Bi. The color map represents the y component of the projected spins contributed by interfacial atomic layers. The green arrows indicate the typical Rashba splitting, where the Rashba coefficient α_R is extracted.

the stacking order of Bi(Ag) and FM is reversed. Therefore, spin current injected from the opposite direction results in opposite charge current in the Fe/Ag/Bi/Py multilayer, consistent with the IREE mechanism at the Bi(Ag)/FM interface albeit exhibiting a peak-and-dip feature. To further confirm this, we subtract the spin pumping curve of YIG/Ag/Bi/Py with that of YIG/Bi/Ag/Fe and find the result indeed is very similar to that of Fe/Ag/Bi/Py (Supplemental Material [37], Note 5), consolidating the above analysis. A comprehensive table as well as a brief description for the criteria to distinguish the ISHE or IREE at different interfaces can be found in Supplemental Material [37], Note 6. We note that, although IREE has been claimed in different FM/NM interfaces [51–54], the IREE at Ag/Bi-FM interfaces has never been considered previously. And we also provided an estimation of effective spin mixing conductance and the inverse Rashba-Edelstein length of different interfaces (Supplemental Material [37], Note 7).

To understand the IREE at the interfaces between Ag/Bi and FMs instead of the Ag/Bi interface itself, we calculate the corresponding interfacial electronic structure based upon density functional theory. Consistent with the study by Ast *et al.* [55] and Bihlmayer, Blügel, and Chulkov [56], our calculation shows the surface states with a giant Rashba splitting of $\alpha_R = 2.92$ eV Å when Ag(111) is doped by 1/3 monolayer of Bi (Supplemental Material [37], Note 8). Such a giant splitting arises from the p_z-dominated surface states localized at the surface alloy monolayer [56]. However, the p_z component can be hybridized with other p bands of Bi with a larger Bi coverage at the surface. The hybridization is considerably enhanced when atomic interdiffusion occurs at the interface. We explicitly calculated the band structure of a disordered interface of Ag/Bi by randomly occupying atoms at the interfacial layers, as shown in Fig. 4(a). Here, owing to the slight intermixing of Ag and Bi atoms, no Rashba-type splitting is found in the vicinity of the Fermi level, indicating the fragility of the giant Rashba splitting of Ag/Bi surface states.

Then we repeat the band structure calculation by modeling a similar disordered interface of Ni/Bi, which is plotted in Fig. 4(b). Strikingly different from the Ag/Bi interface, Rashba-type energy splitting survives at the disordered Ni/Bi interface. Two typical cases are marked by the thick white lines, where the Rashba coefficients $\alpha_R = 1.74$ and 0.96 eV Å are extracted at $E - E_F = 0.8$ and -0.2 eV, respectively. This is because the Bi surface states consist of a mainly p_z component at the outmost layer [56,57], which are hardly affected by the minority-spin d states of Ni near the Fermi level. The hybridization of majority-spin $4s$ state of Ni and p_z surface states of Bi only partially reduces the magnitude of Rashba splitting [56]. The above picture is consistent with the conclusion by a tight-binding model study that the asymmetry of electronic wave functions in both sides of the surface or interface plays an essential role in the quantitative magnitude of Rashba splitting [58]. A specific comparison of projected spin texture near the Fermi energy between clean and disordered Ni/Bi interface is provided in Supplemental Material [37], Note 8, which again confirms that the Rashba splitting at the Ni/Bi interface is less sensitive to the interdiffusion of atoms.

Finally, we study the Ni/Ag interface, where 33% of Ag atoms are replaced by Bi at the interfacial layer inspired by the experimental observation that Bi atoms diffuse till the interface between Ag and FMs (Supplemental Material [37], Note 2). As shown in Fig. 4(c), Rashba energy splitting, $\alpha_R = 2.65$ eV Å, is even larger than those at the Ni/Bi interface, indicating that SOC strength is not the only factor to determine the splitting size. The above electronic structure calculations about the Rashba energy splitting at interfaces qualitatively agree with the phenomena observed in our spin transport experiment that the dominant spin-to-charge conversion via IREE occurs at the interfaces between FMs and the Ag/Bi bilayer.

Our findings provide a coherent picture for the former seemingly contradictory results. The large value of Rashba coefficient reported by angular resolved photoemission spectroscopy [55] is for a relatively sharp Ag/Bi interface only. This Rashba interface can be achieved with submonolayer Bi coverage (Fig. S8 [37]). With further increasing the Bi thickness, the intermixing between Ag and Bi, however, strongly reduces the IREE, resulting negligibly small spin-charge conversion when Ag/Bi is in contact with YIG [33]. A new Rashba interface can be built when Ag/Bi is in contact with a FM, resulting a strong spin-charge conversion [24,25,28,29,31]. As the IREE is dominant at the interface between FM, the spin-charge conversion does not flip its sign when the stacking order of Ag/Bi is reversed [30] and shows a peak-and-dip feature when Ag/Bi is sandwiched by two FMs [34].

In summary, we have performed comprehensive spin pumping measurements for the systems of Bi and Ag/Bi bilayer in contact with both a ferromagnetic insulator (YIG) and ferromagnetic metals (Fe, $Fe_{0.65}Ni_{0.35}$, Py, and Ni) or sandwiched between them. The sign reversal of the spin-charge conversion for the opposite stacking order between Ag/Bi and ferromagnetic metals unambiguously proves the existence of IREE at the interface between them rather than the extensively debated Ag/Bi interface. Electronic structure calculations confirm that both Ni/Bi interface and Bi-doped Ni/Ag interface have significant Rashba splitting, which is attributed to the asymmetry of the electronic wave functions at the interface. In contrast, the Rashba splitting at Ag/Bi interface is sensitively dependent on the interface disorder due to the hybridization of p_z states between Bi and Ag. The finding of IREE between nonmagnetic material and ferromagnetic metals may have strong potential in applications, since the converted pure spin current can exert spin-orbit torque directly onto the ferromagnet without diffusion in the nonmagnetic material. The demonstrated strong tunability of IREE also points a new direction for searching spintronics materials with high efficiency.

This work was supported by the National Key R&D Program of China (Grants No. 2018YFA0306004, No. 2017YFA0303202, and No. 2021YFB3502400), the National Natural Science Foundation of China (Grants No. 51971110, No. 11974165, No. 11734006, No. 11727808, No. 92165103, No. 12004045, No. 12174028, and No. 11734004), and the Natural Science Foundation of Jiangsu Province (Grant No. BK20190057). We thank Professor Xiaofeng Jin from Fudan University for fruitful discussions.

*These authors contribute equally to this work.
†Corresponding author.
bfmiao@nju.edu.cn
‡Corresponding author.
zyuan@bnu.edu.cn
§Corresponding author.
hfding@nju.edu.cn

[1] A. Manchon, H. C. Koo, J. Nitta, S. M. Frolov, and R. A. Duine, Nat. Mater. **14**, 871 (2015).
[2] A. Soumyanarayanan, N. Reyren, A. Fert, and C. Panagopoulos, Nature (London) **539**, 509 (2016).
[3] M. Z. Hasan and C. L. Kane, Rev. Mod. Phys. **82**, 3045 (2010).
[4] P. Narang, C. A. C. Garcia, and C. Felser, Nat. Mater. **20**, 293 (2021).
[5] B. Göbel, I. Mertig, and O. A. Tretiakov, Phys. Rep. **895**, 1 (2021).
[6] W. Han, Y. Otani, and S. Maekawa, npj Quantum Mater. **3**, 27 (2018).
[7] M. Jamali, J. S. Lee, J. S. Jeong, F. Mahfouzi, Y. Lv, Z. Y. Zhao, B. K. Nikolić, K. A. Mkhoyan, N. Samarth, and J.-P. Wang, Nano Lett. **15**, 7126 (2015).
[8] J. E. Hirsch, Phys. Rev. Lett. **83**, 1834 (1999).
[9] S. O. Valenzuela and M. Tinkham, Nature (London) **442**, 176 (2006).
[10] E. Saitoh, M. Ueda, H. Miyajima, and G. Tatara, Appl. Phys. Lett. **88**, 182509 (2006).
[11] D. L. Sun, K. J. van Schooten, M. Kavand, H. Malissa, C. Zhang, M. Groesbeck, C. Boehme, and Z. Valy Vardeny, Nat. Mater. **15**, 863 (2016).
[12] T. Chen, R. K. Dumas, A. Eklund, P. K. Muduli, A. Houshang, A. A. Awad, P. Dürrenfeld, B. G. Malm, A. Rusu, and J. Åkerman, Proc. IEEE **104**, 1919 (2016).
[13] A. A. Awad, P. Dürrenfeld, A. Houshang, M. Dvornik, E. Iacocca, R. K. Dumas, and J. Åkerman, Nat. Phys. **13**, 292 (2017).
[14] L. Q. Liu, C. F. Pai, Y. Li, H. W. Tseng, D. C. Ralph, and R. A. Buhrman, Science **336**, 555 (2012).
[15] L. Q. Liu, O. J. Lee, T. J. Gudmundsen, D. C. Ralph, and R. A. Buhrman, Phys. Rev. Lett. **109**, 096602 (2012).
[16] Y. Cheng, S. S. Yu, M. L. Zhu, J. Hwang, and F. Y. Yang, Phys. Rev. Lett. **124**, 027202 (2020).
[17] R. Urban, G. Woltersdorf, and B. Heinrich, Phys. Rev. Lett. **87**, 217204 (2001).
[18] H. J. Jiao and G. E. W. Bauer, Phys. Rev. Lett. **110**, 217602 (2013).
[19] G. Woltersdorf, M. Buess, B. Heinrich, and C. H. Back, Phys. Rev. Lett. **95**, 037401 (2005).
[20] O. Mosendz, J. E. Pearson, F. Y. Fradin, G. E. W. Bauer, S. D. Bader, and A. Hoffmann, Phys. Rev. Lett. **104**, 046601 (2010).

[21] X. D. Tao, Q. Liu, B. F. Miao, R. Yu, Z. Feng, L. Sun, B. You, J. Du, K. Chen, S. F. Zhang, L. Zhang, Z. Yuan, D. Wu, and H. F. Ding, Sci. Adv. **4**, eaat1670 (2018).

[22] Y. A. Bychkov and É. I. Rashba, JETP Lett. **39**, 66 (1984), http://jetpletters.ru/ps/1264/article_19121.shtml.

[23] V. M. Edelstein, Solid State Commun. **73**, 233 (1990).

[24] J. C. Rojas Sánchez, L. Vila, G. Desfonds, S. Gambarelli, J. P. Attané, J. M. De Teresa, C. Magén, and A. Fert, Nat. Commun. **4**, 2944 (2013).

[25] A. Nomura, T. Tashiro, H. Nakayama, and K. Ando, Appl. Phys. Lett. **106**, 212403 (2015).

[26] S. Sangiao, J. M. De Teresa, L. Morellon, I. Lucas, M. C. Martinez-Velarte, and M. Viret, Appl. Phys. Lett. **106**, 172403 (2015).

[27] W. Zhang, M. B. Jungfleisch, W. Jiang, J. E. Pearson, and A. Hoffmann, J. Appl. Phys. **117**, 17C727 (2015).

[28] H. Nakayama, Y. Kanno, H. An, T. Tashiro, S. Haku, A. Nomura, and K. Ando, Phys. Rev. Lett. **117**, 116602 (2016).

[29] M. B. Jungfleisch, W. Zhang, J. Sklenar, W. Jiang, J. E. Pearson, J. B. Ketterson, and A. Hoffmann, Phys. Rev. B **93**, 224419 (2016).

[30] M. Matsushima, Y. Ando, S. Dushenko, R. Ohshima, R. Kumamoto, T. Shinjo, and M. Shiraishi, Appl. Phys. Lett. **110**, 072404 (2017).

[31] M. B. Jungfleisch, Q. Zhang, W. Zhang, J. E. Pearson, R. D. Schaller, H. D. Wen, and A. Hoffmann, Phys. Rev. Lett. **120**, 207207 (2018).

[32] C. Zhou, Y. P. Liu, Z. Wang, S. J. Ma, M. W. Jia, R. Q. Wu, L. Zhou, W. Zhang, M. K. Liu, Y. Z. Wu, and J. Qi, Phys. Rev. Lett. **121**, 086801 (2018).

[33] D. Yue, W. W. Lin, J. J. Li, X. F. Jin, and C. L. Chien, Phys. Rev. Lett. **121**, 037201 (2018).

[34] J. H. Shen, Z. Feng, P. C. Xu, D. Z. Hou, Y. Gao, and X. F. Jin, Phys. Rev. Lett. **126**, 197201 (2021).

[35] D. Yue, W. W. Lin, and C. L. Chien, APL Mater. **9**, 050904 (2021).

[36] R. Yu, B. F. Miao, Q. Liu, K. He, W. S. Xue, L. Sun, M. Z. Wu, Y. Z. Wu, Z. Yuan, and H. F. Ding, Phys. Rev. B **102**, 144415 (2020).

[37] See Supplemental Material at http://link.aps.org/supplemental/10.1103/PhysRevLett.129.097203 for the details of sample preparation, measurements, and x-ray diffraction; scanning transmission electron microscopy (STEM) characterization; inverse Rashba-Edelstein effect at different Ag/Bi-FM interfaces; the spin diffusion length of $Fe_{0.65}Ni_{0.35}$ alloy and Bi; analysis of the feature for Fe/Ag/Bi/Py; comparison of the different features of ISHE and IREE; estimation of λ_{IREE} of different interfaces; and details of first-principles calculations and spin pumping results for nominal 1/3-ML-Bi/Ag interface, which includes Refs. [38–44].

[38] Y. Niimi, Y. Kawanishi, D. H. Wei, C. Deranlot, H. X. Yang, M. Chshiev, T. Valet, A. Fert, and Y. Otani, Phys. Rev. Lett. **109**, 156602 (2012).

[39] Z. Feng, J. Hu, L. Sun, B. You, D. Wu, J. Du, W. Zhang, A. Hu, Y. Yang, D. M. Tang, B. S. Zhang, and H. F. Ding, Phys. Rev. B **85**, 214423 (2012).

[40] G. Kresse and J. Furthmüller, Phys. Rev. B **54**, 11169 (1996).

[41] P. E. Blöchl, Phys. Rev. B **50**, 17953 (1994).

[42] G. Kresse and D. Joubert, Phys. Rev. B **59**, 1758 (1999).

[43] J. P. Perdew, K. Burke, and M. Ernzerhof, Phys. Rev. Lett. **77**, 3865 (1996).

[44] V. Wang, N. Xu, J.-C. Liu, G. Tang, and W.-T. Geng, Comput. Phys. Commun. **267**, 108033 (2021).

[45] B. F. Miao, S. Y. Huang, D. Qu, and C. L. Chien, Phys. Rev. Lett. **111**, 066602 (2013).

[46] H. L. Wang, C. H. Du, P. C. Hammel, and F. Y. Yang, Appl. Phys. Lett. **104**, 202405 (2014).

[47] D. Z. Hou, Z. Qiu, K. Harii, Y. Kajiwara, K. Uchida, Y. Fujikawa, H. Nakayama, T. Yoshino, T. An, K. Ando, X. F. Jin, and E. Saitoh, Appl. Phys. Lett. **101**, 042403 (2012).

[48] H. Emoto, Y. Ando, G. Eguchi, R. Ohshima, E. Shikoh, Y. Fuseya, T. Shinjo, and M. Shiraishi, Phys. Rev. B **93**, 174428 (2016).

[49] K. He, J. Cheng, M. Yang, Y. H. Zhang, L. Q. Yu, Q. Liu, L. Sun, B. F. Miao, C. M. Hu, and H. F. Ding, Phys. Rev. B **105**, 104406 (2022).

[50] J. Cheng, K. He, M. Yang, Q. Liu, R. Yu, L. Sun, J. J. Ding, B. F. Miao, M. Z. Wu, and H. F. Ding, Phys. Rev. B **103**, 014415 (2021).

[51] D. Fang, H. Kurebayashi, J. Wunderlich, K. Výborný, L. P. Zârbo, R. P. Campion, A. Casiraghi, B. L. Gallagher, T. Jungwirth, and A. J. Ferguson, Nat. Nanotechnol. **6**, 413 (2011).

[52] L. Chen, M. Decker, M. Kronseder, R. Islinger, M. Gmitra, D. Schuh, D. Bougeard, J. Fabian, D. Weiss, and C. H. Back, Nat. Commun. **7**, 13802 (2016).

[53] S. Oyarzún, A. K. Nandy, F. Rortais, J. C. Rojas-Sánchez, M. T. Dau, P. Noël, P. Laczkowski, S. Pouget, H. Okuno, L. Vila, C. Vergnaud, C. Beigné, A. Marty, J. P. Attané, S. Gambarelli, J. M. George, H. Jaffrès, S. Blügel, and M. Jamet, Nat. Commun. **7**, 13857 (2016).

[54] S. Emori, T. Nan, A. M. Belkessam, X. Wang, A. D. Matyushov, C. J. Babroski, Y. Gao, H. Lin, and N. X. Sun, Phys. Rev. B **93**, 180402(R) (2016).

[55] C. R. Ast, J. Henk, A. Ernst, L. Moreschini, M. C. Falub, D. Pacilé, P. Bruno, K. Kern, and M. Grioni, Phys. Rev. Lett. **98**, 186807 (2007).

[56] G. Bihlmayer, S. Blügel, and E. V. Chulkov, Phys. Rev. B **75**, 195414 (2007).

[57] Y. M. Koroteev, G. Bihlmayer, J. E. Gayone, E. V. Chulkov, S. Blügel, P. M. Echenique, and Ph. Hofmann, Phys. Rev. Lett. **93**, 046403 (2004).

[58] L. Petersen and P. Hedegård, Surf. Sci. **459**, 49 (2000).